

A wavelength selective switch for optical add/drop multiplexing of sub-bands within Nyquist WDM super-channels

Bill Corcoran^(1,2), Chen Zhu⁽¹⁾, Jochen Schröder^(2,3), Leimeng Zhuang⁽¹⁾, Benjamin Foo⁽¹⁾, Marizio Burla⁽⁴⁾, Willem P. Beeker⁽⁵⁾, Arne Leinse⁽⁵⁾, Chris G.H. Roeloffzen⁽⁶⁾, Arthur J. Lowery^(1,2)

⁽¹⁾ Monash Electro-Photonics Laboratory, Dept. Electrical and Computer Systems Engineering, Monash University, Clayton, Australia, bill.corcoran@monash.edu

⁽²⁾ Centre for Ultrahigh-bandwidth Devices for Optical Systems (CUDOS), Australia

⁽³⁾ School of Electronic and Computer Systems Engineering, RMIT University, Melbourne, Australia

⁽⁴⁾ Institut National de la Recherche Scientifique (INRS-EMT), Montréal, Canada

⁽⁵⁾ LioniX BV, PO Box 456, Enschede, 7500 AL, the Netherlands

⁽⁶⁾ SATRAX BV, PO Box 456, Enschede, 7500 AL, the Netherlands

Abstract By retrofitting a commercially available WSS with an external photonic integrated circuit module, we demonstrate switching of 12-GHz sub-bands from a Nyquist WDM super-channel. This allows wavelength provisioning in spectrally efficient systems with only a 4% guard-band.

Introduction

Optical super-channels provide a method to increase spectral efficiency in optical links by reducing, or even removing spectral guard-bands. In order for super-channels to be of practical use in modern optically routed networks, a device capable of add/drop multiplexing these closely packed wavelength channels is required. Current wavelength selective switches (WSS) cannot provide the sharp filter responses needed to minimize inter-channel cross-talk; however, only a few methods have been recently proposed to meet this challenge. De-multiplexing of sub-bands within an orthogonal frequency division multiplexed (OFDM) super-channel has been demonstrated using a coherent addition techniques^{1,2}. Ref.² requires high-speed coherent detection, processing and re-transmission for each add/dropped sub-band, while Ref.¹ requires precise clock recovery and timing alignment, so both rely on complex, high-speed electronic feedback circuitry. A sub-GHz resolution proof-of-concept ‘drop’ functionality was shown using an arrayed-waveguide grating as a dispersive element in a liquid crystal on silicon (LCOS) based WSS³. The spectral bandwidth of this device is, however, limited to a 200 GHz operating range³, requiring around 18 separate devices to cover the C-band. A novel

cascaded Mach-Zehnder interferometer photonic-chip recently enabled subchannel demultiplexing of 15% guard-band, 37.5 GHz spaced ‘Nyquist’ wavelength division multiplexing (WDM) super-channel⁴. However, the roll-off of the filters in this device may limit the achievable gains in spectral efficiency.

In this paper, we demonstrate an enhanced WSS, capable of add/drop multiplexing of sub-bands within a Nyquist WDM super-channel with only a 4% guard-band.

The WSS consists of a ring-assisted Mach-Zehnder interferometer (RAMZI) interleaver preceding a commercial 2x1x12 WSS. We show ‘drop’ and ‘continue’ and proof-of-concept, passive ‘add’ functionality. Inter-channel cross-talk generated in the WSS produces <1 dB OSNR penalty at the 7% FEC threshold.

Enhanced WSS architecture

The experimental set-up for the enhanced WSS (EWSS) is shown in Fig. 1a. The incoming super-channel is first launched into a RAMZI interleaver, implemented on a CMOS-process compatible, TriPleX™ silicon nitride chip^{5,6}, configured to provide a 5th-order response using 7 separate biases. The odd and even sub-band outputs are then fed to the two common ports of a 2x1x12 WSS, which then provides the reconfigurable switching. As the RAMZI is used

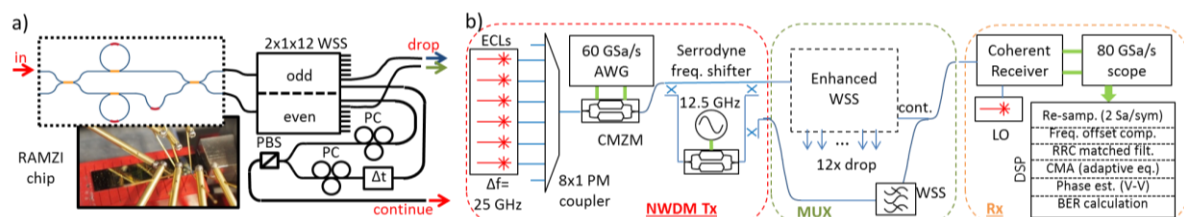


Fig. 1: a) Schematic of enhanced WSS set-up (inset: photo of the RAMZI chip), PC: Polarization controller, PBS: Polarizing beam splitter, Δt : fiber time-delay. b) Experimental system. AWG: Arbitrary waveform generator, ECL: External cavity laser, LO: local oscillator.

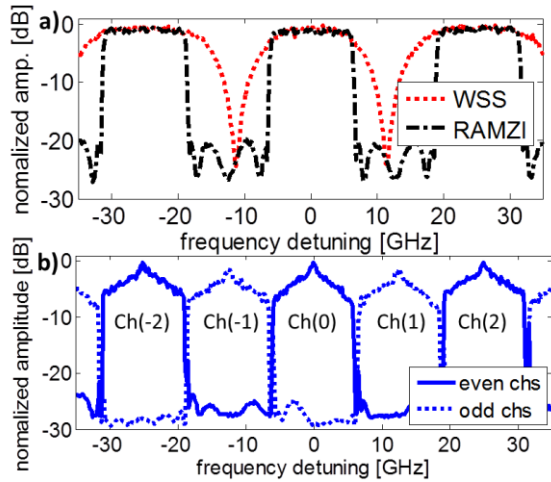


Fig. 2: a) Measured transfer functions for WSS and RAMZI. b) Measured spectra of odd and even data channels at the enhanced WSS outputs. Both spectra are centred at 193.1055 THz, with sub-bands labelled as in (b).

as an interleaver before the WSS, we avoid the limitation to operation over only a single free-spectral range, unlike the arrangement found in Ref. ³. This enables us, in principle, to cover the entire C-band with a single device.

The processed odd and even sub-bands after the WSS are recombined with a 3-dB optical coupler, with the odd sub-bands delayed by ≈ 10 ns to de-correlate the signals and inter-channel cross-talk. As such, each sub-band experiences the maximum degradation from cross-talk. The polarisation controllers and a polarising beam splitter are only required to ensure odd and even sub-band polarisation alignment at the output, as the chip transmits only in a single polarisation. This is unnecessary for dual-polarisation operation, by using two separate RAMZIs on-chip for polarization diversity, achievable since the RAMZI filter structure occupies < 20 mm² (including resistive heaters and contact pads).

The channel response of the WSS and RAMZI, measured with a 15-MHz resolution spectrometer (Agilent 83453B), are shown in Fig. 2a. The RAMZI shows adjacent sub-band rejection down to -20 dB, with the WSS providing further suppression. Fig. 2b shows the measured spectra of the optical signal at the output of the EWSS, with neighbouring channels well isolated. From this measured spectrum the expected signal-to-interference ratio is 21.0 dB, calculated as the total in-band signal power from the odd port to total in-band interference power coupled in from the even port. The insertion losses of the RAMZI chip and WSS are 9 dB and 5 dB respectively.

System performance

Fig. 1b shows the system experiment. A 20-GHz bandwidth complex Mach-Zehnder modulator

(CMZM) modulates the optical carriers from 6 ECLs, spaced 25-GHz apart, with 12-Gbaud QPSK using Nyquist pulse shaping with a 0.01 roll-off, digital root-raised cosine (RRC) filter with 20-dB stopband attenuation. Pre-emphasis at the transmitter is neglected in favour of adaptive matched filtering at the receiver side. A portion of the optical signal is serrodyne frequency shifted⁷ by 12.5 GHz, and delayed to de-correlate the data between the frequency shifted and original components. These two components are then recombined to create a 150-GHz wide, 4% guard-band Nyquist WDM super-channel.

Prior to processing in the EWSS, the super-channel signal is noise loaded with amplified spontaneous emission. The EWSS's output is amplified and optically filtered (40 GHz bandwidth) before coherent detection. The receiver output is digitized with a real-time, 80 GSa/s, 33-GHz bandwidth oscilloscope, and offline processed. The digital signal processing flow resamples to 2 Sa/symb, applies spectrum-based frequency offset compensation, then RRC matched filtering. A constant-modulus algorithm based adaptive equalizer and a Viterbi-Viterbi phase estimator are used before bit-error rate (BER) calculation.

Fig. 1b also shows the emulation of 'add' functionality through passive combination, in order to allow us to demonstrate the viability of our EWSS in a reconfigurable add/drop multiplexer (ROADM) architecture. Here, a single sub-band is isolated out of the modulated, 25-GHz spaced band by power splitting and filtering with a WaveShaper, delayed to de-correlate with the super-channel, and added back with the EWSS processed super-channel to replace a dropped sub-band. As such, the set-up allows us to demonstrate the viability of simultaneous, reconfigurable 'add' and 'drop' functions using the EWSS.

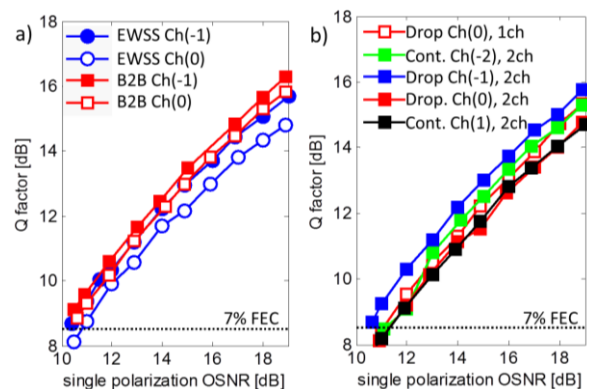


Fig 3: Measured Q vs. OSNR for: a) back-to-back (B2B) and post-EWSS set to continue all sub-bands; b) 'Drop' and neighbouring 'Continue' (Cont.) sub-bands with one or two sub-bands dropped. Sub-band numbering is as per Fig. 3b).

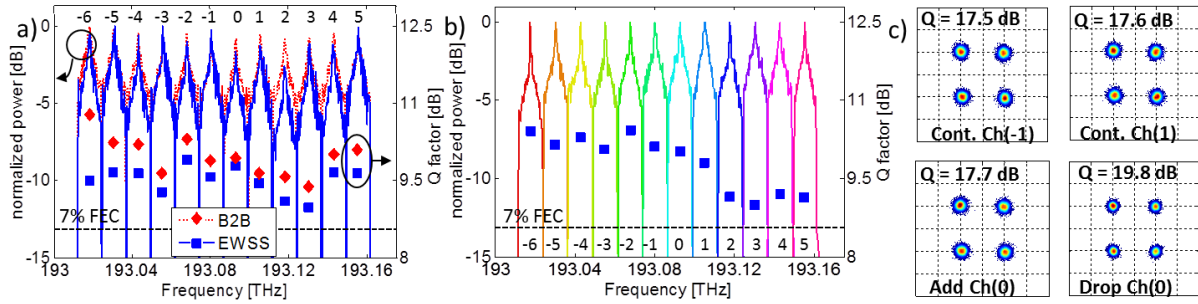


Fig. 4: Spectra and Q measurements for: a) all sub-bands set to continue and b) for sub-bands dropped to separate WSS ports, each color denoting a different port. Blue squares and red diamonds are for post-EWSS and B2B cases, respectively. OSNR = 11.5 dB. c) Received constellations for ‘drop’, ‘continue’ and passive ‘add’ sub-bands after mux. OSNR > 20 dB.

Fig. 3a shows the performance of the EWSS with all sub-bands set to continue. A small OSNR penalty due to the EWSS of ≈ 0.4 dB measured for both sub-bands at the 7% FEC threshold. Signal quality factor (Q) is plotted for back-to-back (B2B) configuration and with the full EWSS in place. In this ‘all-continue’ case, the EWSS splits then re-combines the now decorrelated odd and even sub-bands, so a penalty is expected. At low OSNRs, where there are >100 errors measured, Q from error-vector magnitude ($Q = -20\log_{10}(\text{EVM}[\text{lin.}])$) matches well with Q_{BER}^2 derived from BER as $20\log_{10}(2^{0.5}\text{erfc}^{-1}[2\text{BER}])$. An Q of 8.53 dB equates to the 7% hard FEC (RS{255,239}) threshold.

Fig. 3b shows system performance when the EWSS is set to drop 1 or 2 sub-bands. The performance for the dropped (Chs. -1 and 0) and neighbouring continue sub-bands (Chs. -2 and 1) is plotted against OSNR. The dropped and the continued sub-bands have similar performance near the FEC threshold, with required OSNR varying within 0.8 dB.

Fig. 4a shows Q for all sub-bands of the super-channel, with the EWSS set to ‘all-continue’, and OSNR=11.5 dB. The band-to-band variation for back-to-back and post-EWSS Qs are similar (± 0.7 dB for B2B, ± 0.5 dB post-WSS), with a reduction in Q due to the EWSS of between 0.2 and 0.9 dB. Fig. 4b shows that the system can de-multiplex 12 sub-bands to 12 separate WSS outputs; the sub-bands’ Qs only vary by ± 0.7 dB.

Fig. 4c demonstrates the potential for simultaneous ‘add’ and ‘drop’ functionality in the system, showing the constellations and extracted Q values of the nearest neighbour continue sub-bands, the passively added sub-band within the super-channel, and the isolated ‘drop’ sub-band. In B2B, $Q \approx 20$ dB without noise loading, limited by interference from the frequency shifting stage. Without noise loading, the Q of the ‘continue’ and passive ‘add’ sub-bands are within 0.1 dB of 17.6 dB, with the ‘drop’ sub-band at 19.8 dB. This shows that the

‘continue’ and passive ‘add’ sub-bands all experience similar cross-talk. The ‘drop’ sub-band is isolated from the super-channel before re-combination and so is not distorted by inter-channel interference, as reflected in its higher Q.

Conclusions

We have demonstrated a WSS architecture capable of reconfigurable optical ‘add’, ‘drop’ and ‘continue’ functionality for sub-bands within a Nyquist WDM super-channel with only 4% guard-band, utilizing passive optical filtering only. OSNR sweeps show <1dB penalties at the 7% FEC threshold due to inter-channel cross-talk, demonstrating the utility of this device for transparent optical networks employing ultrahigh-bandwidth super-channels.

Acknowledgements

This work was supported by Laureate Fellow (LF130100041), DECRA (DE120101329) and Centres of Excellence (CE110001018) schemes of the Australian Research Council. We thank Finisar Australia for the $2 \times 1 \times 12$ WSS.

References

- [1] S.J. Fabbri et al., “Full Experimental Implementation of an All-Optical Interferometric Drop, Add, and Extract Multiplexer for Superchannels,” *J. Lightwave Technol.*, Vol. **33**, p. 1351 (2015).
- [2] T. Richter et al., “Coherent In-line Substitution of OFDM Subcarriers Using Fiber-Frequency Conversion and Free-Running Lasers,” *Proc. OFC*, Th5B.6, San Francisco (2014).
- [3] R. Rudnick et al., “Sub-Banded / Single-Sub-Carrier Drop-Demux and Flexible Spectral Shaping with a Fine Resolution Photonic Processor” *Proc. ECOC*, PD.4.1, Cannes (2014).
- [4] T. Goh et al., “Optical Nyquist-Filtering Multi/Demultiplexer with PLC for 1-Tb/s Class Super-Channel Transceiver” *Proc. OFC*, Tu3A.5, Las Angeles (2015).
- [5] L. Zhuang et al., “Ring-based interleaver for Nyquist filtering and WDM multiplexing” *Proc. OFC*, Tu3A.6, Las Angeles (2015).
- [6] C. G. H. Roeloffzen et al., “Silicon nitride microwave photonic circuits”, *Opt. Express*, Vol. **21**, p. 22937 (2013)
- [7] M. Izutsu et al., “Integrated optical SSB modulator/frequency shifter” *J. Quant. Electron.*, vol. **17**, p. 2225 (1981)